ACS Macro Letters

Letter

pubs.acs.org/macroletters

Dynamics and Rheology of Soft Colloidal Glasses

Yu Ho Wen, Jennifer L. Schaefer, and Lynden A. Archer*

School of Chemical and Biomolecular Engineering, Cornell University, Ithaca, New York 14853, United States

Supporting Information

ABSTRACT: The linear viscoelastic (LVE) spectrum of a soft colloidal glass is accessed with the aid of a time−concentration superposition (TCS) principle, which unveils the glassy particle dynamics from in-cage rattling motion to out-of-cage relaxations over a broad frequency range 10^{-13} rad/s < ω < 10^{1} rad/s. Progressive dilution of a suspension of hairy nanoparticles leading to increased intercenter distances is demonstrated to enable continuous mapping of the structural relaxation for colloidal glasses. In contrast to existing empirical approaches proposed to extend the rheological map of soft glassy materials, i.e., time−strain superposition (TSS) and strain−rate frequency superposition (SRFS), TCS yields a LVE master curve that satisfies the Kramers−Kronig relations which interrelate the dynamic moduli for materials at equilibrium. The soft glassy rheology (SGR) model and literature data further support the general validity of the TCS concept for soft glassy materials.

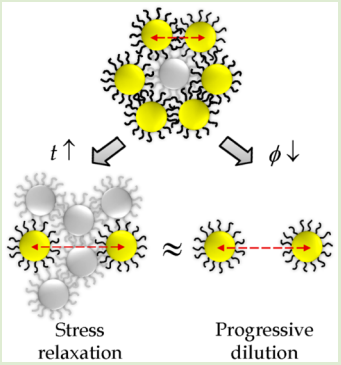

Under the influence of thermal forces alone, a moderately concentrated suspension of particles of size a in an equilibrium, unentangled polymeric fluid is able to explore all of its configuration space in a time scale of the order $\lambda_{eq} \approx 6\pi\eta a^3/k_BT$ set primarily by the bulk viscosity η of the polymer host. It should be emphasized that this situation prevails even though each individual particle in the suspension must continuously escape temporary entrapments in short-lived cages defined by the close proximity of their neighbors. Increasing the particle concentration above a critical value drives the system to a jammed state in which the particles are disordered on long length scales; however, the cages are long-lived, and the particle equilibration time diverges as does the overall suspension viscosity.[1−6] Softening the particles by tethering polymer chains to their surface provides an effective means of lowering the particle volume fraction at which the glass transition is observed[2,7] and of facilitating short-range adjustments of individual particle positions (i.e., in-cage motions) that in some cases allow even a jammed suspension of particles to exhibit no/negligible evidence of aging.[8] These relaxation processes are analogous to so-called β-relaxations in molecular and polymeric glasses and are readily evidenced by fast decay of particle correlations in dynamic light scattering.[4,5,9]

Despite fundamental differences in glassy relaxation behaviors observed in colloidal glasses and molecular glass-forming liquids,[6,10−12] it has long been understood that glass formation in model colloidal suspensions can provide insight into the physics of molecular glasses.[3,6,13] Linear viscoelasticity near the glass transition has been investigated for a variety of soft colloidal systems, such as polymerically stabilized particles,[5,14−16] charged particles,[17] colloidal star polymers,[18−20] microgel particles,[7,21,22] etc. Mode-coupling theory (MCT)[5,6,14,16,23−26] and soft glassy rheology (SGR) theory[1,27−30] have provided good frameworks for describing glassy dynamics in these systems. It is now known that in colloidal glasses the probability of escaping from the cage depends on the extent of jamming or cage dimensions (number of particles constraining the test particle), and the time required for observing complete cage escape may be of geological time scales.[8] As a consequence, very little is known about the mechanisms through which particles escape their cages or about the processes whereby the rubber-like plateau seen in the linear viscoelastic spectrum gives way to terminal relaxation.

Various empirical methods have been proposed in the recent literature to access the terminal relaxation of soft glassy materials. In an analogous manner to time−temperature superposition (TTS),[31,32] a time−strain superposition (TSS) approach has for instance been used to create rheological maps of suspension dynamics that cover unprecedented time scales.[8,33] In particular, by imposing an external perturbation sufficiently large to overcome the energy barrier associated with the caging it was shown that dynamic moduli measured over a finite range of frequency and at different, large strain amplitudes can be overlaid to form an approximately continuous time map that captures the uncaging transition. A strain−rate frequency superposition (SRFS) was proposed even earlier to create the master curve by superposing dynamic moduli obtained in a limited frequency range, yet at multiple fixed effective shear rates $\dot{\gamma}$ (= $\gamma\omega$).[34,35] Because both TSS and SRFS access the terminal regime in a driven material, the master curves thus obtained violate the Kramers−Kronig relations which interconvert the storage (G') and loss (G'') moduli for materials at equilibrium. Additionally, SRFS was found to significantly overestimate the rate of terminal relaxation for kinetically arrested suspensions. Thus, the relevance of the information

Received: October 19, 2014
Accepted: December 30, 2014
Published: January 7, 2015

DOI: 10.1021/mz5006662
ACS Macro Lett. 2015, 4, 119−123

uncovered by these methods to the understanding of quiescent glasses is debatable.[36,37] Alternatively, a time−concentration or time−composition superposition (TCS) principle has long been used in conjunction with small-amplitude oscillatory shear (SAOS) measurements to extend the rheological map for entangled polymers,[38−41] triblock copolymers,[42] microgels,[7] and particle suspensions,[38,40,43] by overlying G' and G'' data measured at multiple concentrations, with respect to a reference fluid state that may be chosen at any concentration. In a previous publication we demonstrated that suspensions with particle concentrations that bracket the liquid-to-glass transition obey an analogous TCS superposition principle that allows a complete master curve for their relaxation dynamics to be constructed, providing access to in-cage glassy dynamics as well as dynamics at the uncaging transition.[38]

In this Letter we study dynamics of a model soft colloidal glass and elucidate the physics that produce TCS. By carefully examining the TCS master curves in both frequency and time domains and comparing the shift factors with expectations from linear viscoelastic theories we find that TCS is a fundamental characteristic of soft glasses. We show that with sufficient care in experiment design it should always be possible to empirically characterize the full relaxation spectrum of a jammed soft colloidal glass. Indeed, because the suspension concentration sets the interparticle spacing prior to jamming and also largely determines the state of compression of tethered chains after jamming, TCS in reality provides a way to sample different cage energies—and hence cage-escape probabilities—and as such is a powerful, but heretofore essentially unexplored, analogue to the TTS method for studying dynamics of complex fluids. These points are made more concrete with the help of the SGR model, where we show that any experimental design that allows the cage strength of a soft glass to be systematically manipulated can be used in conjunction with experiments in the linear viscoelastic regime to recover the full relaxation spectrum.

We study a model soft colloid consisting of SiO_2 nanoparticles (LUDOX SM-30, Sigma-Aldrich) densely grafted with polyethylene glycol (PEG) oligomers (~1.2 chain/nm^2; $M_{PEG} \approx 550$ g/mol). The average diameter of the uncoated silica nanoparticles was determined to be 10 ± 2 nm from the form-factor analysis of small-angle X-ray scattering (SAXS) intensity profiles.[30,44] The synthesis of the PEG-silica particles and procedures for suspension preparation were reported previously.[30,38] The suspending medium used here is a Newtonian fluid, comprised of unentangled mPEG oligomers (methoxy polyethylene glycol; $M_{mPEG} \approx 350$ g/mol) of similar chemistry as the tethered PEG ligands. The suspending medium also has a similar refractive index to silica, thereby reducing van der Waals attractions between silica cores and preventing wholesale aggregation, as revealed by our SAXS structure-factor analyses.[30,45] As already established in previous studies,[30,45] these suspensions exhibit exceptional colloidal stability, and even in the jammed state, their dynamic moduli are virtually invariant with time (see Supporting Information). Characterization by low-stress creep experiments reveals a Newtonian flow regime at low shear rates in the suspensions (Supporting Information). These structural and rheological features are understood to come from the reorientation of tethered PEG ligands, which facilitates short-range particle motions, analogous to arm retraction of colloidal star polymers.[20]

PEG-silica nanoparticle suspensions with a range of SiO_2 core volume fractions (ϕ_c = 0.20−0.40) were subjected to small-amplitude oscillatory shear (SAOS) using an Anton Paar MCR 301 rheometer outfitted with cone-and-plate fixtures (10 mm diameter and 4° cone angle; 25 mm diameter and 1° cone angle; 50 mm diameter and 1° cone angle). As shown in Figure 1, the frequency dependence of G' and G'' reveals a clear

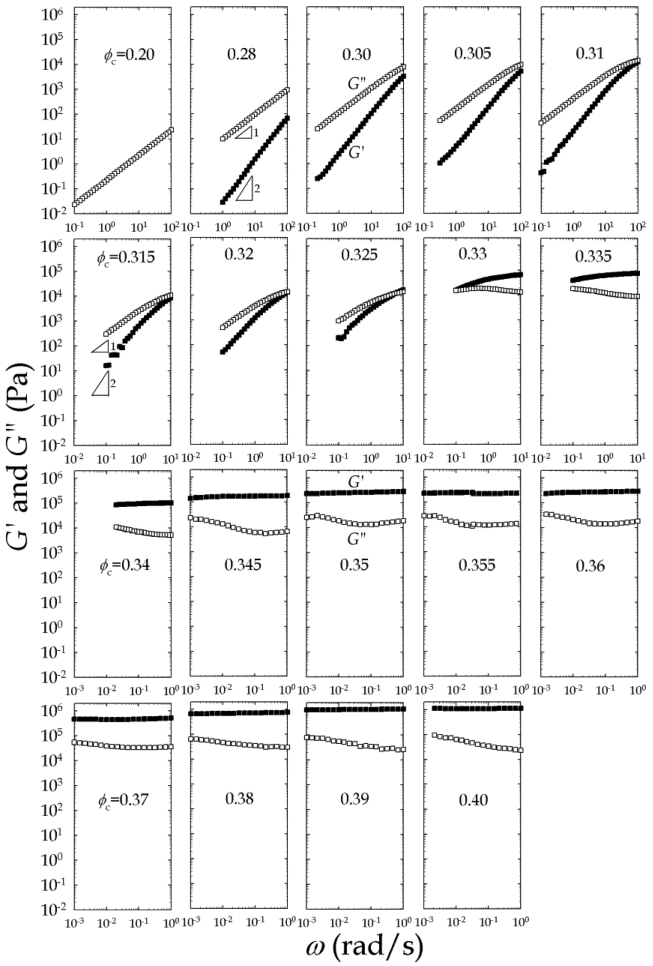

Figure 1. Frequency dependence of G' and G'' in a range of silica core volume fractions from ϕ_c = 0.20 to 0.40 at 40 °C.

transition from a liquid state ($G' \sim \omega^2$ and $G'' \sim \omega$) to a glassy state ($G' \sim \omega^0$) with increasing ϕ_c. The time scale of cage escape, associated with the crossover frequency at which $G' = G''$, can be seen to increase by several orders of magnitude over the concentration range. The rubbery plateau develops, and the zero-shear-rate viscosity begins to rise very rapidly upon a critical SiO_2 core volume fraction $\phi_c^* \approx 0.33$ (Supporting Information), where particle crowding starts to restrict motion.

The critical core volume fraction identified above should correspond to the liquid-to-glass transition $\phi_g \approx 0.58$ generally reported for hard-sphere colloids,[1−3,7] which interact as a result of excluded volume. Thus, at $\phi_c^* \approx 0.33$ the densely grafted PEG corona increases the effective volume fraction of the silica core and yields an apparent brush height H = 1.0 ± 0.2 nm, where the relation $\phi_g = \phi_c^*(1 + H/a)^3$ is used.[46] Near the liquid-to-glass transition, the brush height is noted to be close to half of the intersurface distance determined from SAXS (d_{ss} =1.5 ± 0.1 nm; inset of Figure 2a), where the interparticle distance d_{pp} is estimated from the first interaction peak of the structure factor using $d_{pp} \approx 2\pi/q$. The observation that the

DOI: 10.1021/mz5006662
ACS Macro Lett. 2015, 4, 119−123

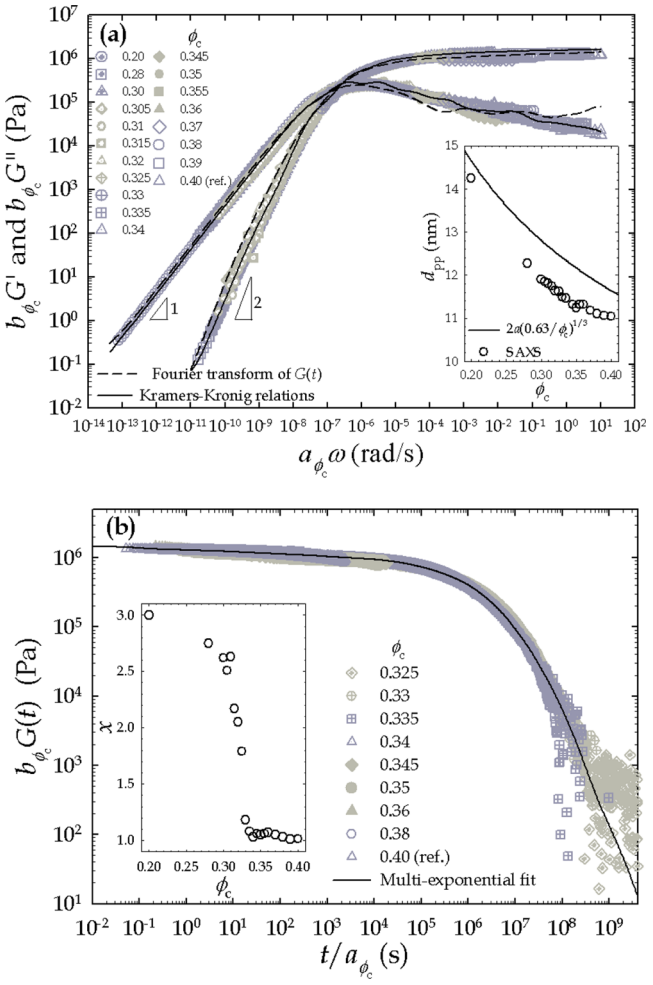

Figure 2. Time−concentration superposition (TCS) master curves obtained, respectively, in the frequency (a) and time (b) domains for a reference PEG-silica colloidal glass with $\phi_c = 0.40$. Insets in (a) and (b) show the concentration dependences of SAXS-determined interparticle distance d_{pp} and noise temperature x, respectively.

brush height is comparable to the intersurface distance suggests that not only are the particles well dispersed in the concentrated suspensions, but also the tethered PEG chains are confined and compressed. After the transition, the tethered ligands begin to interpenetrate and impose long-lived topological constraints on the cores, leading to jamming (or kinetic arrest). The jammed structure can be broken down by large-amplitude oscillatory shear (LAOS), when the imposed stress/strain exceeds a critical value, as evidenced by a pronounced maximum in the first harmonic of $G''(\gamma)$ (Supporting Information).[46] The $G''(\gamma)$ maximum indicates liquid-like behavior and results from energy dissipation associated with cage breakup.[47]

To further quantify the extent of jamming for the individual suspensions shown in Figure 1, we retrieve the so-called noise temperature x from the linear viscoelastic spectra in a fixed frequency range of 0.01 to 1 rad/s, using the soft glassy rheology (SGR) model prediction, $G' \sim \omega^{x-1}$ for $1 < x < 3$,[28] as summarized in the inset of Figure 2b. In the SGR model, the noise temperature can be thought of as the energy available for a trapped particle to hop out of its cage formed by surrounding particles. The inset shows that above the critical core volume fraction $\phi_c^* \approx 0.33$ the noise temperatures approach 1 because G' becomes virtually independent of frequency, suggestive of complete jamming and the formation of a colloidal glass. Additionally, as noted previously,[38,48] the rubbery plateaus saturate at a value close to the melt plateau modulus of entangled poly(ethylene oxide) (PEO) polymers of the same chemistry as the tethered PEG ligands ($G_{e,PEO} \approx 1.8 \times 10^6$ Pa at 80 °C).[31] This suggests that the jamming results from the highly interpenetrating, topologically constrained PEG ligands; it is the short-range motion of these ligands that appears to relax residual stresses and virtually eliminates aging of the jammed materials.

The ratio of G'/G'' attains a high value of around 50 at the highest suspension concentration ($\phi_c \approx 0.40$), and therefore the elasticity completely dominates the suspension rheology. These observations, all together, indicate that upon approaching the concentration $\phi_c^* \approx 0.33$ the PEG-silica nanoparticle suspensions have approached a glassy state, but for short-range in-cage rattling motions facilitated by the dynamics of the tethered PEG ligands, motion of the particles is arrested.

The main results of this Letter are summarized in Figure 2a, where a smooth linear viscoelastic (LVE) master curve is created by horizontal and vertical shifting of the G' and G'' data sets displayed in Figure 1 ($\phi_c = 0.20$−0.39), with respect to a reference colloidal glass ($\phi_c = 0.40$). The horizontal (a_{ϕ_c}) and vertical (b_{ϕ_c}) shift factors are summarized in Figure 3 and will

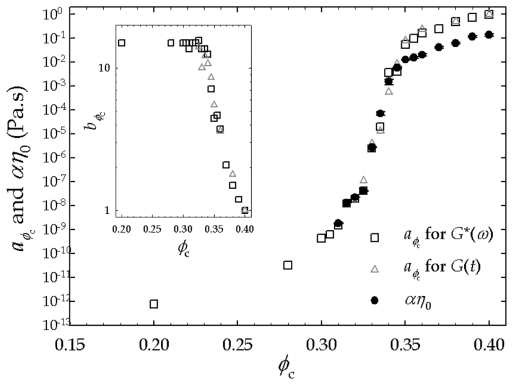

Figure 3. Concentration dependences of horizontal (a_{ϕ_c}) and vertical (b_{ϕ_c}) shift factors for dynamic modulus $G^*(\omega)$ and relaxation modulus $G(t)$ in Figure 2. Zero-shear-rate viscosity η_0 is scaled by a factor $\alpha = 4 \times 10^{-12}$ to superpose onto the values of a_{ϕ_c} at low concentrations.

be discussed shortly. The resultant TCS master curve in Figure 2a is by almost any measure remarkable in terms of its ability to substantially extend the frequency range—10^{-13} rad/s < ω < 10^{1} rad/s—over which the detailed relaxation dynamics of the colloidal glass can be observed. Specifically, the LVE spectrum clearly shows a transition from a rubbery plateau to a terminal relaxation regime with decreased frequency (or increased observation time).

In Figure 2a the nearly frequency-independent loss modulus G'' in the rubbery plateau regime (10^{-2} rad/s < ω < 10^{0} rad/s) is thought to reflect the in-cage rattling motion (β-relaxation) of the particles discussed previously, and the frequencies are associated with the fundamental exploration time for in-cage motion and as such may be analogous to the entanglement Rouse time, τ_e, for long, entangled polymer chains constrained to diffuse in a tube. After the crossover frequency ($\omega_c \approx 10^{-6.5}$ rad/s) the jammed particles escape the cages, and familiar

DOI: 10.1021/mz5006662
ACS Macro Lett. 2015, 4, 119−123

scaling relationships $G' \sim \omega^2$ and $G'' \sim \omega$ known for an isotropic, equilibrium state of relaxed complex fluids are recovered.[6] This finding is consistent with the observation that the zero-shear-rate viscosity η_0 of the jammed suspensions remains measurable using creep experiments at shear rates smaller than 10^{-6} 1/s (Supporting Information). The longest material relaxation time, presumably the cage escape time τ_{cage}, can be estimated from the reciprocal of the crossover frequency ω_c, and the estimate reveals the very large time scale required for the colloidal glass to attain an equilibrium state, i.e., $\tau_{cage} \approx 10^{6.5}$ s $\approx$ 36 days. τ_{cage} may also be estimated as the inverse of the critical shear rate at which shear thinning commences in a steady-shear creep measurement. This approach yields an estimate for the apparent terminal relaxation time, $\tau_{cage} \approx \dot{\gamma}_c^{-1} \approx$ 12 days. The agreement is not exact, but shows that the extraordinary slow particle dynamics revealed by the simple TCS procedure are meaningful in understanding other rheological behaviors of a jammed suspension.

Considering that all oscillatory shear experiments used to create the master curve are performed in the linear viscoelastic regime, we expect that the dynamic moduli $G^*(\omega) = G'(\omega) + iG''(\omega)$ should satisfy the Kramers−Kronig relations which interconvert the real and imaginary parts of the stress response to a harmonic excitation.[47] On the basis of a good analytical fit for either moduli (29 relaxation modes; not shown), we verify in Figure 2a that it is able to predict the other using the Kramers−Kronig relations (solid lines). The good agreement confirms that the TCS master curve is the linear rheological response of the colloidal glass. Similar rich dynamics of a glassy suspension should be accessible from small-amplitude step-strain experiments performed in the time domain. Figure 2b reports a composite linear stress relaxation modulus $G(t)$ obtained using TCS on relaxation data obtained using the same suspensions employed in the oscillatory shear experiments. Fourier transformation of the resultant $G(t)$ yields dynamic moduli that compare favorably with the TCS master curve (dashed lines). The agreement between the data in the time and frequency domains is taken for granted for simple fluids in the linear viscoelastic regime and can also be considered additional justification for the use of TCS to map extended relaxation dynamics for soft colloidal glasses. To assess the generality of the approach we have applied TCS in a similar manner to other soft materials, including entangled polymers,[38] hairy particles,[38] colloidal star polymers,[19] and microgels;[7] master curves obtained for a representative set of these materials are provided as Supporting Information. We also remark that, using the SGR model without taking into account rheological aging phenomena,[29] a theoretical TCS master curve can be created in a similar fashion from the calculated G' and G'' data sets (at $x = 1-3$ in small increments) because the transition to a glass can be brought about by increasing the cage strength (see Supporting Information for additional details).

The horizontal (a_{ϕ_c}) and vertical (b_{ϕ_c}) shift factors used in constructing the TCS master curves in Figures 2a (frequency domain) and 2b (time domain) are summarized in Figure 3. The arguments in the introduction justifying TCS imply that the horizontal shift factor a_{ϕ_c} is proportional to the terminal relaxation time of the suspension, i.e., $a_{\phi_c} \sim \tau_{cage}$. Thus, a dramatic change of a_{ϕ_c} near the glass transition ($\phi_c^* \approx 0.33$) can be considered a signal for an abrupt increase in the cage lifetime and hence approach of the glassy state, where particles begin to undergo kinetic arrest. We further expect the cage escape time τ_{cage} to be related to the terminal viscosity by the formula, $\tau_{cage} = \eta_0/G'_\infty$. We also note that the high-frequency limit of G'_∞ is at best only weakly dependent on concentration, which means that another scaling relationship should hold, i.e., $a_{\phi_c} \sim \tau_{cage} \sim \eta_0$. This expectation is tested in Figure 3 where η_0, shifted vertically by a concentration-independent constant factor α, is compared with a_{ϕ_c} obtained from application of TCS in the frequency and time domains. It is apparent that η_0 changes significantly near the liquid-to-glass transition and can be overlaid with a_{ϕ_c} over much of the concentration range studied. The agreement is least good for the most concentrated suspensions, where wall slip and other effects can compromise the quality of the measured η_0 in creep. However, even this level of agreement is remarkable considering the large differences in the measurement time scale. This is another justification of the TCS principle for unveiling extremely slow dynamics of soft colloidal glasses, whose long-time structural relaxation can be mimicked from the suspension rheology of diluted suspension with increasing intercenter distances. Additionally, the scaling suggests that self-similar particle dynamics exist in the suspensions as ϕ_c is increased.

Consistent with the horizontal shift factor, the vertical shift factor b_{ϕ_c} shown in the inset of Figure 3 shows a sudden change upon the liquid-to-glass transition. Since b_{ϕ_c} reflects the variation of the strength of the particle networks (i.e., plateau modulus) with particle concentration, the change is thought to reflect an increase in the entanglement density produced by more interdigitated ligands. Comparing the concentration dependences of b_{ϕ_c} and zero-shear-rate viscosity, we find that over the particle concentration range investigated the plateau modulus increases by as much as ∼15 times, whereas the viscosity rises more than 10 decades, implying that the compressed tethered chains have stronger impacts on dynamics in comparison to rheological properties.

It is known that the transition toward a glass in suspensions is driven by increasing the particle concentration. The TCS concept is therefore analogous to the commonly used TTS, for which at $T > T_g$ the temperature-dependent shift factors are generally described by the empirical William−Landel−Ferry (WLF) equation.[31] We therefore devise a WLF analogue for analyzing the concentration-dependent shift factors (a_{ϕ_c}) required to construct the TCS master curve (see Supporting Information for additional details). The analysis suggests a similar linear (concentration) dependence of the free volume as embedded in the original WLF equation until the suspensions become jammed (i.e., $\phi_c^* \approx 0.33$ as identified earlier), after which the free volume is anticipated to approach zero faster than predicted by the Doolittle equation, presumably as a result of the interdigitation of tethered ligands and high loading of hard silica cores.

In summary, considering PEG-silica nanoparticles as a model soft colloidal system in which the soft corona facilitates density fluctuations and short-range relaxation of the hard cores, we find that a time−concentration superposition (TCS) principle can be exploited to create a continuous map of the complete dynamic response of soft colloidal glasses on time scales ($t > 10^8$ s) inaccessible from real-time experiments. The success of the approach demonstrates that in colloidal glasses structural relaxation from in-cage rattling motion to the subsequent out-of-cage motion can be mimicked by progressively diluting the material, leading to increased mean intercenter distances. In

DOI: 10.1021/mz5006662
ACS Macro Lett. 2015, 4, 119−123

other words, the particles that have lost their spatial correlation can act as diluents for unrelaxed particles. We also find that the TCS concept seems valid for a variety of soft glassy materials and is supported by the soft glassy rheology (SGR) model. Unlike the existing time−strain superposition (TSS) and strain−rate frequency superposition (SRFS) principles used for constructing rheological maps using nonlinear oscillatory data (i.e., out of equilibrium states), TCS allows access to a master curve obeying the Kramers−Kronig relations and hence provides a very powerful means of probing extremely slow particle dynamics for soft glassy materials.

■ ASSOCIATED CONTENT

Ⓢ Supporting Information

Additional rheological characterization and data analyses. This material is available free of charge via the Internet at http://pubs.acs.org.

■ AUTHOR INFORMATION

Corresponding Author

*E-mail: laa25@cornell.edu (L.A.A.).

Notes

The authors declare no competing financial interest.

■ ACKNOWLEDGMENTS

This work was supported by the National Science Foundation, Award No. DMR-1006323 and by Award No. KUS-C1-018-02, made by King Abdullah University of Science and Technology (KAUST). Facilities available through the Cornell Center for Materials Research (CCMR) were used for this study. The SAXS experiments were conducted at the Cornell High Energy Synchrotron Source (CHESS) which is supported by the National Science Foundation and the National Institutes of Health/National Institute of General Medical Sciences under NSF award DMR-1332208.

■ REFERENCES

(1) Joshi, Y. M. *Annu. Rev. Chem. Biomol. Eng.* **2014**, *5*, 181−202.
(2) Pusey, P. N.; van Megen, W. *Nature* **1986**, *320*, 340−342.
(3) Hunter, G. L.; Weeks, E. R. *Rep. Prog. Phys.* **2012**, *75*, 066501.
(4) Ozon, F.; Petekidis, G.; Vlassopoulos, D. *Ind. Eng. Chem. Res.* **2006**, *45*, 6946−6952.
(5) Brambilla, G.; El Masri, D.; Pierno, M.; Berthier, L.; Cipelletti, L.; Petekidis, G.; Schofield, A. B. *Phys. Rev. Lett.* **2009**, *102*, 085703.
(6) Larson, R. G. *The Structure and Rheology of Complex Fluids*; Oxford University Press: New York, 1999.
(7) Mattsson, J.; Wyss, H. M.; Fernandez-Nieves, A.; Miyazaki, K.; Hu, Z.; Reichman, D. R.; Weitz, D. A. *Nature* **2009**, *462*, 83−86.
(8) Agarwal, P.; Qi, H.; Archer, L. A. *Nano Lett.* **2010**, *10*, 111−115.
(9) Pusey, P. N.; van Megen, W. *Phys. Rev. Lett.* **1987**, *59*, 2083−2086.
(10) Di, X.; Peng, X.; McKenna, G. B. *J. Chem. Phys.* **2014**, *140*, 054903.
(11) Di, X.; Win, K. Z.; McKenna, G. B.; Narita, T.; Lequeux, F.; Pullela, S. R.; Cheng, Z. *Phys. Rev. Lett.* **2011**, *106*, 095701.
(12) McKenna, G. B.; Narita, T.; Lequeux, F. *J. Rheol.* **2009**, *53*, 489−516.
(13) Winter, H. H. *Macromolecules* **2013**, *46*, 2425−2432.
(14) Siebenbürger, M.; Fuchs, M.; Winter, H.; Ballauff, M. *J. Rheol.* **2009**, *53*, 707−726.
(15) Mason, T. G.; Weitz, D. A. *Phys. Rev. Lett.* **1995**, *75*, 2770−2773.
(16) Crassous, J. J.; Casal-Dujat, L.; Medebach, M.; Obiols-Rabasa, M.; Vincent, R.; Reinhold, F.; Boyko, V.; Willerich, I.; Menzel, A.; Moitzi, C.; Reck, B.; Schurtenberger, P. *Langmuir* **2013**, *29*, 10346−10359.
(17) Negi, A. S.; Osuji, C. O. *Phys. Rev. E* **2010**, *82*, 031404.
(18) Helgeson, M. E.; Wagner, N. J.; Vlassopoulos, D. *J. Rheol.* **2007**, *51*, 297−316.
(19) Erwin, B. M.; Cloitre, M.; Gauthier, M.; Vlassopoulos, D. *Soft Matter* **2010**, *6*, 2825−2833.
(20) Vlassopoulos, D. *J. Polym. Sci., Part B: Polym. Phys.* **2004**, *42*, 2931−2941.
(21) Koumakis, N.; Pamvouxoglou, A.; Poulos, A. S.; Petekidis, G. *Soft Matter* **2012**, *8*, 4271−4284.
(22) Zhou, Z.; Hollingsworth, J. V.; Hong, S.; Cheng, H.; Han, C. C. *Langmuir* **2014**, *30*, 5739−5746.
(23) van Megen, W.; Underwood, S. M. *Phys. Rev. E* **1994**, *49*, 4206−4220.
(24) Brader, J. M.; Voigtmann, T.; Fuchs, M.; Larson, R. G.; Cates, M. E. *Proc. Natl. Acad. Sci. U.S.A.* **2009**, *106*, 15186−15191.
(25) Götze, W.; Sjögren, L. *Chem. Phys.* **1996**, *212*, 47−59.
(26) Wolfgang, G. *J. Phys.: Condens. Matter* **1999**, *11*, A1−A45.
(27) Sollich, P. *Phys. Rev. E* **1998**, *58*, 738−759.
(28) Sollich, P.; Lequeux, F.; Hébraud, P.; Cates, M. E. *Phys. Rev. Lett.* **1997**, *78*, 2020−2023.
(29) Fielding, S. M.; Sollich, P.; Cates, M. E. *J. Rheol.* **2000**, *44*, 323−369.
(30) Srivastava, S.; Shin, J. H.; Archer, L. A. *Soft Matter* **2012**, *8*, 4097−4108.
(31) Rubinstein, M.; Colby, R. H. *Polymer Physics*; Oxford University Press: New York, 2003.
(32) Fox, T. G.; Flory, P. J. *J. Am. Chem. Soc.* **1948**, *70*, 2384−2395.
(33) Agarwal, P.; Archer, L. A. *Phys. Rev. E* **2011**, *83*, 041402.
(34) Wyss, H. M.; Miyazaki, K.; Mattsson, J.; Hu, Z.; Reichman, D. R.; Weitz, D. A. *Phys. Rev. Lett.* **2007**, *98*, 238303.
(35) Mohan, P. H.; Bandyopadhyay, R. *Phys. Rev. E* **2008**, *77*, 041803.
(36) Erwin, B. M.; Rogers, S. A.; Cloitre, M.; Vlassopoulos, D. *J. Rheol.* **2010**, *54*, 187−195.
(37) Hess, A.; Aksel, N. *Phys. Rev. E* **2011**, *84*, 051502.
(38) Wen, Y. H.; Lu, Y.; Dobosz, K. M.; Archer, L. A. *Macromolecules* **2014**, *47*, 4479−4492.
(39) Baumgärtel, M.; Willenbacher, N. *Rheol. Acta* **1996**, *35*, 168−185.
(40) Daga, V.; Wagner, N. *Rheol. Acta* **2006**, *45*, 813−824.
(41) Schausberger, A.; Ahrer, I. V. *Macromol. Chem. Phys.* **1995**, *196*, 2161−2172.
(42) Krishnan, A. S.; Spontak, R. J. *Soft Matter* **2012**, *8*, 1334−1343.
(43) Trappe, V.; Weitz, D. A. *Phys. Rev. Lett.* **2000**, *85*, 449−452.
(44) Yu, H.-Y.; Srivastava, S.; Archer, L. A.; Koch, D. L. *Soft Matter* **2014**, *10*, 9120−9135.
(45) Srivastava, S.; Archer, L. A.; Narayanan, S. *Phys. Rev. Lett.* **2013**, *110*, 148302.
(46) Mewis, J.; Wagner, N. J. *Colloidal Suspension Rheology*; Cambridge University Press: New York, 2012.
(47) Tschoegl, N. W. *The Pnenomenological Theory of Linear Viscoelastic Behavior: An Introduction*; Springer: New York, 1989.
(48) Agarwal, P.; Kim, S. A.; Archer, L. A. *Phys. Rev. Lett.* **2012**, *109*, 258301.

DOI: 10.1021/mz5006662
ACS Macro Lett. 2015, 4, 119−123